Initiation of tRNA maturation by RNase E is essential for cell viability in *E. coli*

Maria C. Ow and Sidney R. Kushner[1]

Department of Genetics, University of Georgia, Athens, Georgia 30602, USA

RNase E, an essential endoribonuclease in *Escherichia coli*, is involved in 9S rRNA processing, the degradation of many mRNAs, and the processing of the M1 RNA subunit of RNase P. However, the reason that RNase E is required for cell viability is still not fully understood. In fact, recent experiments have suggested that defects in 9S rRNA processing and mRNA decay are not responsible for the lack of cell growth in RNase E mutants. By using several new *rne* alleles, we have confirmed these observations and have also ruled out that M1 processing by RNase E is required for cell viability. Rather, our data suggest that the critical in vivo role of RNase E is the initiation of tRNA maturation. Specifically, RNase E catalytic activity starts the processing of both polycistronic operons, such as *glyW cysT leuZ*, *argX hisR leuT proM*, and *lysT valT lysW valZ lysY lysZ lysQ*, as well as monocistronic transcripts like *pheU*, *pheV*, *asnT*, *asnU*, *asnV*, and *asnW*. Cleavage by RNase E within a few nucleotides of the mature 3′ CCA terminus is required before RNase P and the various 3′ → 5′ exonucleases can complete tRNA maturation. All 59 tRNAs tested involved RNase E processing, although some were cleaved more efficiently than others.

[*Key Words*: mRNA decay; rRNA processing; RNase P; RNase G; RNase T]

Received February 8, 2002; revised version accepted March 27, 2002.

Ribonuclease E (RNase E) of *Escherichia coli* was first characterized in a temperature-sensitive mutant (*rne-3071*) that accumulated 9S precursors of the 5S rRNA at 42°C (Ghora and Apirion 1978). Independently, the *ams* (altered mRNA stability) gene was identified because of its ability to affect the decay of total pulse-labeled RNA at elevated temperatures (Ono and Kuwano 1979). Subsequently, both loci were shown to encode RNase E (Mudd et al. 1990; Babitzke and Kushner 1991; Taraseviciene et al. 1991). The *rne* gene encodes a 1061-amino-acid protein (Casarégola et al. 1992, 1994) that has now been characterized as a 5′-end-dependent endoribonuclease (Mackie 1998). In addition, it has also been shown that RNase E is part of a multiprotein complex, called the degradosome, that includes polynucleotide phosphorylase (PNPase), the RhlB RNA helicase, and the glycolytic enzyme enolase (Carpousis et al. 1994; Py et al. 1994, 1996; Miczak 1996).

In vivo experiments with either the *rne-1* or *rne-3071* temperature-sensitive alleles have shown the accumulation of unprocessed 5S rRNA intermediates (Ghora and Apirion 1978; Babitzke et al. 1993) and a general slowing in the decay of specific mRNA transcripts (Arraiano et al. 1988; Mackie 1991; Régnier and Hajnsdorf 1991). As such it was assumed that the inviability associated with the inactivation of RNase E resulted from a defect in either 9S rRNA processing or mRNA decay. However, experiments by López et al. (1999) and Ow et al. (2000) suggest that this hypothesis is not correct. For example, using *rne* deletion mutations, both laboratories showed that 9S rRNA processing was almost normal under conditions in which mRNA decay was significantly impaired (López et al. 1999; Ow et al. 2000). Furthermore, Ow et al. (2000) characterized an extensive RNase E C terminus truncation mutation (*rneΔ610*) that was missing 609 amino acids, including the ARRBS (arginine-rich RNA-binding site) and the degradosome scaffolding region (Fig. 1). This protein was able to support cell viability at 37°C but not at 44°C. More importantly, decay of specific mRNAs was more defective at 37°C than in an *rne-1* mutant shifted to the nonpermissive temperature. Therefore, it was concluded that inviability in the absence of RNase E was not associated with defects in either mRNA decay or 9S rRNA processing (Ow et al. 2000).

Accordingly, we have sought to determine what other aspect of RNA metabolism requires the activity of this enzyme. One possibility was a defect in the processing of the M1 RNA subunit of RNase P (Gurevitz et al. 1983; Lundberg and Altman 1995). Because this is the only enzyme in *E. coli* that can generate the mature 5′ termini of tRNAs, the loss of its activity leads to cell inviability. However, because M1 RNA containing extra nucleotides at its 3′ terminus still retains catalytic activity (Liu and Altman 1995), this did not seem to be a likely explanation.

[1]Corresponding author.
E-MAIL skushner@arches.uga.edu; FAX (706) 542-3910.
Article and publication are at http://www.genesdev.org/cgi/doi/10.1101/gad.983502.

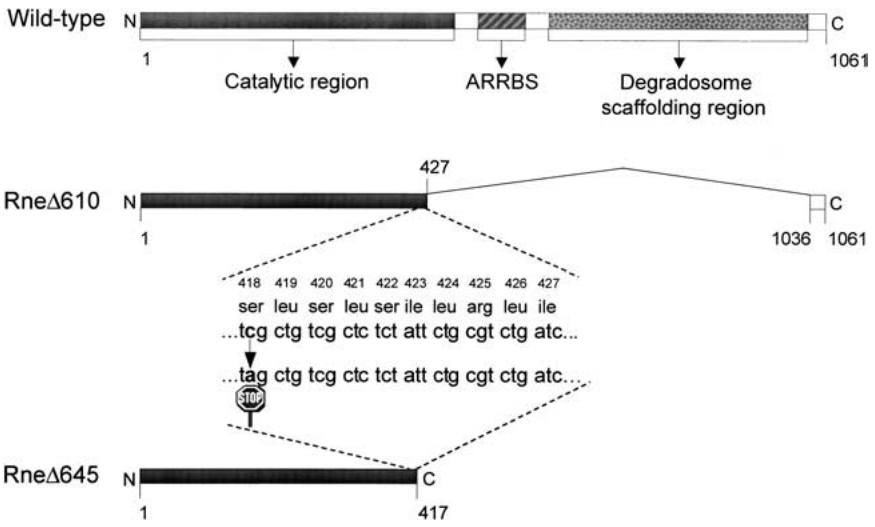

Figure 1. Schematic representation of the *rne*$^+$, *rne*Δ*610*, and *rne*Δ*645* alleles. The *rne*Δ*610* mutation encodes a truncated RNase E protein encompassing the first 427 amino acids of the N terminus plus the last 25 amino acids of the C terminus (Ow et al. 2000). The *rne*Δ*645* revertant contains a C → A transversion on serine 418 (T**C**G → T**A**G), creating a premature stop codon to generate an RNase E polypeptide with only the first 417 amino acids of the N terminus. The various domains of the wild-type RNase E protein are as described by Vanzo et al. (1998). The figure is not drawn to scale.

A more attractive candidate was tRNA processing. The *E. coli* genome contains 86 tRNAs, many of which exist in polycistronic operons (Berlyn 1998). Although these transcripts could be processed by a combination of endonucleolytic cleavage by RNase P at the 5′ end (Altman et al. 1995) and exonucleolytic degradation at the 3′ end by RNase II, RNase BN, RNase PH, RNase D, RNase T, and PNPase (Li and Deutscher 1996), it is also possible that RNase E is required to cleave within the intercistronic regions. Failure to process tRNAs properly would lead to a cessation of protein synthesis and concomitantly cell growth. In fact, Ono and Kuwano (1979) observed a drop-off in the rate of protein synthesis when an *rne-1* strain (called *ams-1* at that time) was shifted to the nonpermissive temperature. In addition, when Ray and Apirion (1981b) isolated small RNAs from an *rne-3071* mutant shifted to 42°C, they found 9S rRNA precursors as well as molecules that contained both tRNA^{Leu} and tRNA^{His}. These two tRNAs are part of a four-gene tRNA transcription unit, *argX hisR leuT proM* (Berlyn 1998). Subsequently, they showed that if such tRNA precursors were treated in vitro with RNase E, then RNase P could cleave at the 5′ end (Ray and Apirion 1981a).

Using a series of RNase E mutants, we have examined the relationships among RNase E function, tRNA processing, and cell viability. Of particular importance was the fortuitous isolation of a temperature-resistant revertant of the *rne*Δ*610* allele (Ow et al. 2000), called *rne*Δ*645*. The *rne*Δ*645* mutation encodes an RNase E protein of only 417 amino acids, but unlike *rne*Δ*610*, permits cell growth at both 37°C and 44°C. Whereas the processing of both polycistronic and monocistronic tRNAs was impaired at 44°C in *rne-1*, *rne*Δ*610*, and *rne*Δ*645* strains, transcripts matured 2.9- to 3.7-fold faster in the *rne*Δ*645* mutant compared with the *rne-1* and *rne*Δ*610* strains. There was a direct correlation among tRNA processing rates, the steady-state levels of mature tRNAs, and cessation of cell growth. In addition, RNase P cleavage at the 5′ end of tRNA transcripts was dependent on prior RNase E processing at the 3′ terminus.

Results

Isolation and characterization of rneΔ645, *a temperature-resistant revertant of the* rneΔ610 *allele*

Because of our interest in mRNA decay, we constructed an *rng::cat rne*Δ*610* double mutant (SK9982). When this strain was replica-plated to 44°C, a small number of temperature-resistant revertants were identified. Of eight that were tested, one (SK9987) arose from an alteration in the plasmid carrying the *rne*Δ*610* allele. DNA sequencing of the complete *rne* gene in pMOK21 revealed a single nucleotide change, a C → A transversion within the codon for serine 418, resulting in a stop codon (Fig. 1). This new premature stop codon further shortened the protein from the RneΔ610 parent by 35 amino acids, generating a polypeptide, RneΔ645, of 417 amino acids that migrated as an ~46-kD protein in an 8% SDS polyacrylamide gel (Figs. 1, 2). The autoregulation of RNase E synthesis, a phenomenon first described by Jain and Belasco (1995), was completely lost in the *rne*Δ*645* strain (Fig. 2, lane 4). A similar loss of autoregulation has been observed previously with the *rne*Δ*610* allele (Fig. 2, lane 3; Ow et al. 2000). To confirm that the C → A transversion was responsible for the suppression of lethality observed in SK9987, we used site-directed mutagenesis to reconstruct the *rne*Δ*645* mutation in pMOK15 (*rne*Δ*610* Cm^r), creating pMOK29 (*rne*Δ*645* Cm^r). Transformation of pMOK29 into SK9705 and the subsequent displacement of the resident plasmid (pQLK26, *rne*$^+$ Km^r) resulted in a strain, SK10103, whose properties were identical to SK9987.

Growth properties of the rneΔ645 *mutant*

On Luria agar medium at 44°C, SK9987 (*rne*Δ*645*) took 2 d to form large colonies compared with 1 d for the *rne*$^+$ control (SK9714). In Luria broth, SK9987 continued to grow at 44°C (35 min generation time), albeit more slowly than the wild-type SK9714 control (26 min; Fig. 3A). In contrast, SK9957, the *rne*Δ*610* progenitor, ceased growing at ~4 h after the shift to the nonpermissive tem-

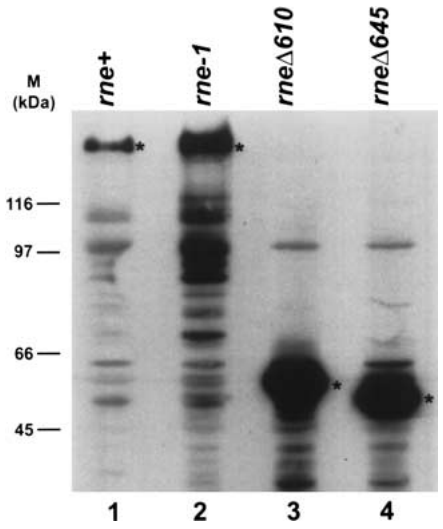

Figure 2. Western analysis of various RNase E proteins. Equivalent amounts of total protein lysates (50 µg) were electrophoresed in an 8% SDS/PAGE gel and electrotransferred onto an Immobilon PVDF membrane (Millipore). Membranes were probed for RNase E as described in Materials and Methods. Size standards are on the left. Asterisks denote the full-length RNase E proteins. (Lane *1*) SK9714; (lane *2*) SK9937; (lane *3*) SK9957; (lane *4*) SK9987.

perature (Fig. 3A). A control strain, SK9937, harboring the *rne-1* temperature-sensitive allele ceased growing between 60 and 90 min after the shift to 44°C (Fig. 3A).

Because these strains contained low-copy-number plasmids (6–8 copies/cell) carrying the *rne*$^+$, *rne-1*, *rne*Δ*610*, and *rne*Δ*645* alleles, we also determined the growth properties of cells carrying these mutations in a single copy. To accomplish this, the *rne*$^+$, *rne-1*, *rne*Δ*610*, and *rne*Δ*645* alleles were moved into pMOK40 (Ow et al. 2002), a single-copy vector carrying Sm^r/Sp^r. Under these conditions, both the *rne-1* and *rne*Δ*610* strains ceased growing at ~120 min after the shift to 44°C, whereas the *rne*Δ*645* and *rne*$^+$ strains continued growing (Fig. 3B). Interestingly, the increased copy number of the *rne-1* allele caused a more rapid cessation of cell growth (cf. SK9937 and SK10144 in Fig. 3A,B). In contrast, the generation times for the *rne*Δ*645* strains at 44°C were 35 min (SK9987, 6–8 copies) versus 47 min (SK2685, single-copy). Based on Western blot analysis, there was a three-to fourfold decrease in the amount of the RneΔ610 and RneΔ645 proteins when the mutations were present in the single-copy plasmid compared with the 6–8-copy-number plasmid (data not shown).

mRNA decay properties of the rneΔ645 *mutant*

Previous analysis of the *rne*Δ*610* allele had suggested that the conditional lethality associated with the *rne-1* and *rne-3071* mutations was not related to defects in mRNA decay (Ow et al. 2000). To determine if this hypothesis were correct, we examined the decay of two RNase E-dependent transcripts, *rpsT* and *rpsO* (Mackie 1991; Hajnsdorf et al. 1994) at both 37°C and 44°C in the *rne*Δ*645* mutant. At 37°C, both the *rpsO* and *rpsT* mRNAs decayed between 1.5- and 1.7-fold more rapidly in SK9987 (*rne*Δ*645*) than in SK9957 (*rne*Δ*610*), but their decay rates were still much slower than those obtained in *rne*$^+$ and *rne-1* strains (Table 1A). In fact, the half-lives in the *rne*Δ*645* strain at 37°C were still equal to or longer than those observed in an *rne-1* mutant at the nonpermissive temperature (Ow et al. 2000).

We also determined the half-lives of the *rpsO*, *rpsT*, and *pnp* transcripts at 44°C in strains carrying single copies of the *rne*Δ*610* and *rne*Δ*645* alleles (Table 1B). Under these conditions, mRNA decay in the *rne*Δ*645* strain was either more defective than in the *rne-1* mutant (*rpsO*) or not significantly better (*rpsT* and *pnp*; Table 1B). It should also be noted that with all three transcripts, the half-lives increased considerably in the *rne*Δ*610* strain relative to *rne-1*, even though the *rne-1* strain ceased growing sooner at 44°C (Fig. 3B). In contrast, the half-lives of all three transcripts in the *rne*Δ*645* mutant were comparable to those observed in the *rne-1* strain even though it continued growing at 44°C (Fig. 3B; Table 1).

Comparison of 9S rRNA processing in the rneΔ610 *and* rneΔ645 *mutants*

Because we had previously observed that 9S rRNA processing was relatively normal in the *rne*Δ*610* mutant (Ow et al. 2000), we did not expect to see a significant difference between the *rne*Δ*610* and *rne*Δ*645* strains. To confirm this prediction, we probed a Northern blot containing total RNA, isolated from *rne*$^+$, *rne-1*, *rne*Δ*610*, and *rne*Δ*645* strains that had either been grown at 37°C or had been shifted to 44°C for 150 min, with an oligonucleotide complementary to 5S rRNA. As expected, in the *rne-1* strain, larger rRNA precursors accumulated when the strain was shifted from 37°C to 44°C (Fig. 4). In contrast, there were significantly fewer precursors in both the *rne*Δ*610* and *rne*Δ*645* mutants at 44°C (Fig. 4). In fact, the steady-state levels of mature 5S rRNA were identical in the wild-type, *rne*Δ*610*, and *rne*Δ*645* strains at 44°C compared with a 32% reduction in the *rne-1* mutant (Fig. 4).

Comparison of M1p processing in the rneΔ610 *and* rneΔ645 *mutants*

It has been shown that RNase E is involved in the maturation of the M1 RNA subunit of RNase P (Gurevitz et al. 1983; Lundberg and Altman 1995). Because this enzyme is required for the generation of the mature 5′ ends of tRNAs (Altman et al. 1995), we determined the half-life of the M1 precursor (M1p) in the *rne*Δ*610* and *rne*Δ*645* strains to ascertain whether a change in the processing of this transcript could account for the difference in cell growth at 44°C (Fig. 3A,B). In the *rne*$^+$ control, processing occurred too rapidly to determine a half-life (Table 2). In contrast, when the *rne-1*, *rne*Δ*610*, and *rne*Δ*645* alleles were present in 6–8 copies/cell, the half-life of the M1p was identical within experimental error (Table 2). When the *rne* alleles were present in single

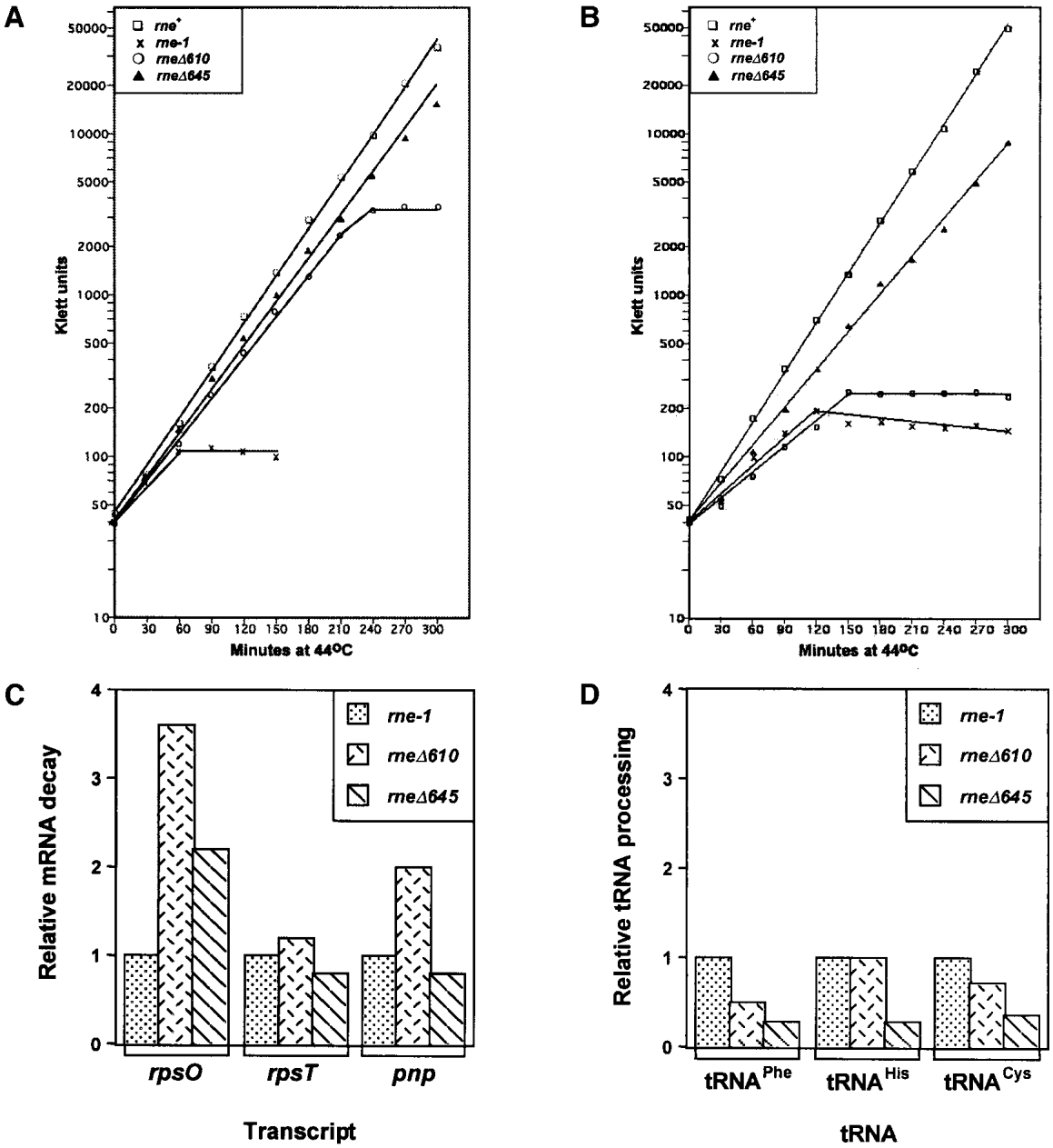

Figure 3. Comparison of the growth properties, mRNA decay rates, and tRNA processing rates of strains carrying the *rne*$^+$, *rne-1*, *rne*Δ*610*, and *rne*Δ*645* alleles in either 6–8 copies/cell or single copy. Growth curves were carried out as described in Materials and Methods. (*A*) Growth curve with 6–8 copies/cell of each *rne* allele. (*B*) Growth curve with each *rne* allele in single copy. (*C*) Relative mRNA half-lives as a function of RNase E activity. (*D*) Relative tRNA precursor half-lives as a function of RNase E activity. The half-life of each mRNA (Table 1) and the half-life of each tRNA precursor obtained with the specific 3′-oligonucleotide probe (Table 3) in the *rne-1* strain was set at 1.

copy, the M1p half-life in the *rne-1* and *rne*Δ*645* strains was almost identical, whereas it was almost four times longer in the *rne*Δ*610* mutant (Table 2).

Processing of polycistronic transcripts containing tRNAs and tRNAs encoded within rRNA operons requires functional RNase E activity

Because the changes in mRNA decay rates as well as 9S rRNA and M1 processing did not seem sufficient to account for the ability of the *rne*Δ*645* strain to grow at 44°C, we next analyzed the processing of tRNAs in *rne*$^+$, *rne-1*, *rne*Δ*610*, and *rne*Δ*645* strains at 44°C. If RNase E were required for tRNA processing, we assumed that its most likely role would be in the cleavage of polycistronic operons that contained several tRNAs. Initially, we chose to analyze the *glyW cysT leuZ* (Fig. 5A) and *argX hisR leuT proM* polycistronic transcripts (data not shown) because the *cysT* and *hisR* genes are unique.

Using an oligonucleotide probe (cysT–leuZ), we car-

Table 1. *mRNA half-lives at 37°C and 44°C*

Transcript A	Half-life (min)[a]			
	rne$^+$	*rne-1*[b]	*rneΔ610*	*rneΔ645*
rpsO[c]	1.8 ± 0.4	2.9 ± 0.3	16.3 ± 1.7	9.4 ± 2.1
rpsT[c]	1.5 ± 0.1	2.3 ± 0.4	4.4 ± 0.3	2.9 ± 0.0
Transcript B	*rne*$^+$	*rne-1*[b]	*rneΔ610*	*rneΔ645*
rpsO[c]	ND	8.4 ± 1.0	>30	18.7 ± 4.0
rpsT[c]	ND	5.0 ± 1.4	6.1 ± 1.3	3.8 ± 0.3
pnp	ND	10.0 ± 1.2	>20	8.4 ± 1.0

Half-lives for transcript A were determined at 37°C in strains carrying the various alleles in 6–8 copies/cell. Half-lives for transcript B were determined in strains carrying the various alleles in single copy after cultures had been shifted to 44°C for 120 min.
[a]The data represent the average of two independent determinations.
[b]*rne-1* encodes a temperature sensitive RNase E protein that is unable to support cell viability at 44°C (Ono and Kuwano 1979; Babitzke and Kushner 1991). RNase E activity is partially inactivated at 37°C (Ow et al. 2000).
[c]For *rpsO,* the half-life of the *rpsO2* transcript (Ow et al. 2000) is presented. For *rpsT,* the half-life is the average of the two major transcripts (Mackie 1991).
ND, Not determined.

ried out a half-life experiment for the intercistronic region between the *cysT* and *leuZ* genes (Fig. 5A,B). Although no precursor transcripts were visible in the wild-type control, two large species of 460 (full length) and 290 nucleotides (nt) were observed in the *rne-1*, *rneΔ610*, and *rneΔ645* mutants, along with a series of smaller intermediates ranging in size from 90 to 200 nt (Fig. 5B). Half-life determinations for the largest species showed that the *rneΔ645* strain processed it twofold faster than the *rneΔ610* mutant and 2.8-fold faster than the *rne-1* strain (Table 3; Fig. 3D). As a control, the membrane was stripped and reprobed for the mature tRNA^{Cys} (Fig. 5D).

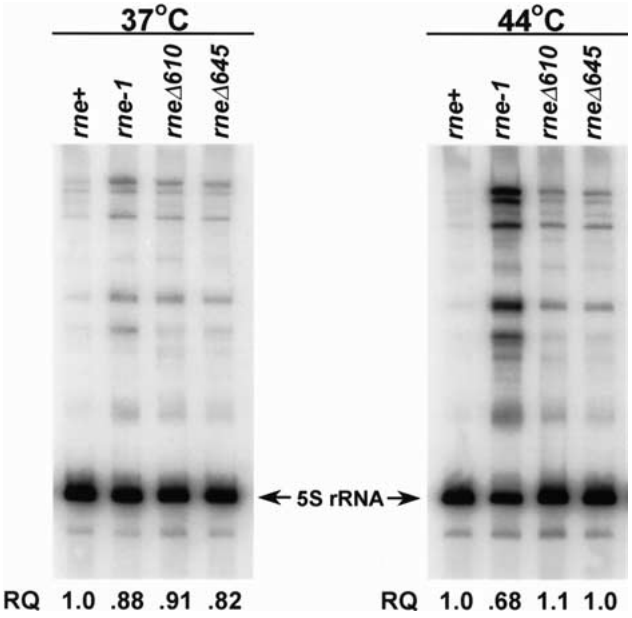

Figure 4. Northern analysis of 9S rRNA processing. Five micrograms of total steady-state RNA isolated from either 37°C or 44°C as described in Materials and Methods was separated on a 6% PAGE/7 M urea gel, electrotransferred onto a nylon membrane (MSI MagnaCharge; Osmonics), and probed with a ^{32}P-5′-end-labeled oligonucleotide complementary to the 5S rRNA (PB5S rRNA). The arrows indicate the 5S rRNA; the larger species are processing intermediates. RQ is the amount of mature 5S rRNA in each strain compared with the wild-type control.

Table 2. *Half-lives[a] of the M1 precursor of RNase P in various strains at 44°C*

Copy number	Genotype			
	rne$^+$	*rne-1*	*rneΔ610*	*rneΔ645*
6–8	ND	20.8 ± 6.0	20.1 ± 1.3	22.5 ± 10.9
1	ND	23.2[b]	87.6 ± 12.7	19.1 ± 2.4

[a]Data represent the average of two independent determinations. Cultures were grown at 37°C until they reached ~1 × 10^8 cells/mL and were then shifted to 44°C. After 150 min of growth, half-life determinations (in minutes) were carried out as described in Materials and Methods.
[b]This experiment was performed once only.
ND, The M1 precursor was not detected in the wild-type strain.

To confirm that these observations were not unique to the *glyW cysT leuZ* operon, we next tested the *argX hisR leuT proM* polycistronic transcript. A probe (hisR–leuT) for the spacer region between *hisR* and *leuT* detected two large precursor transcripts of 530 (full length) and 335 nt in addition to smaller species between 85 and 225 nt in length in the *rne* mutants (data not shown). Again, no precursors were seen in the wild-type control. With this operon, the decay of the full-length precursor was almost identical in the *rne-1* and *rneΔ610* strains (Table 3; Fig. 3D) and much slower than that observed for the *glyW cysT leuZ* operon. However, the processing in the *rneΔ645* strain was 3.7-fold faster than in either the *rne-1* or *rneΔ610* mutants (Table 3; Fig. 3D).

We also examined whether RNase E was involved in the processing of tRNA operons that contained multiple copies of specific tRNAs. For these experiments we chose the *tyrT tyrV tpr* and *lysT valT lysW valZ lysY lysZ lysQ* operons. In both cases, significant amounts of processing intermediates were observed in the three *rne* mutants compared with none in the wild-type control (data not shown). Similar differences in tRNA processing were observed when the *rneΔ610* and *rneΔ645* alleles were present in single copy (data not shown). As a final experiment, we tested the four *glt* tRNAs because they are all contained within rRNA operons (*rrnB*, *rrnC*, *rrnE*, and *rrnB*). As was seen with polycistronic tRNA transcripts, functional RNase E activity was required to obtain mature tRNA^{Glt} (data not shown).

Processing of monocistronic tRNA transcripts also requires functional RNase E activity

Because monocistronic transcripts have relatively short 3′ ends, we assumed that the multiple 3′ → 5′ exonucle-

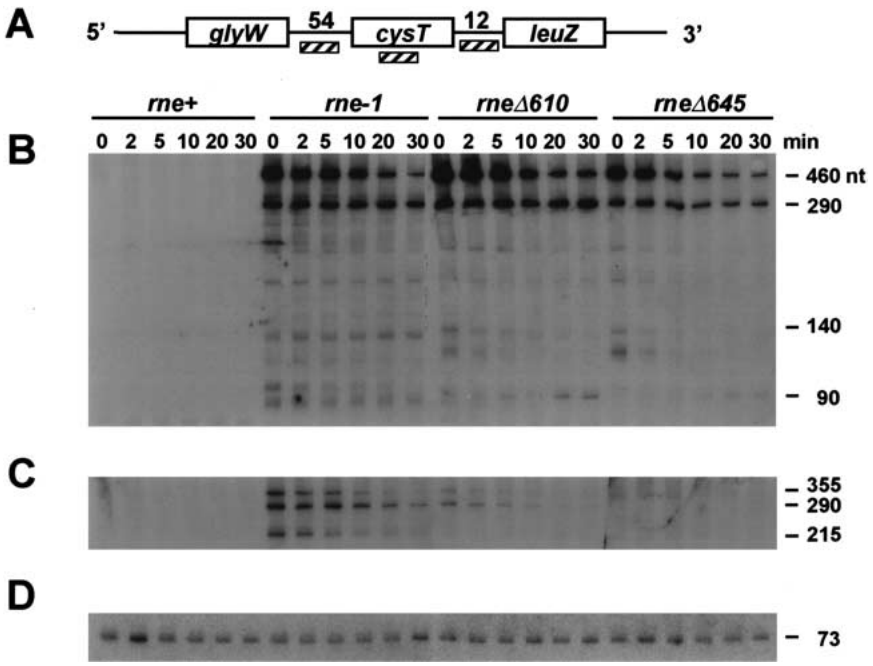

Figure 5. Processing of the *glyW cysT leuZ* polycistronic transcript. Cultures were grown in LB medium at 44°C as described in Materials and Methods. Ten micrograms of total RNA isolated from SK9714 (*rne*$^+$), SK9937 (*rne-1*), SK9957 (*rne*Δ*610*), and SK9987 (*rne*Δ*645*) at 0, 2, 5, 10, 20, and 30 min after rifampicin addition was loaded in each lane. The RNA samples were electrophoresed on a 6% PAGE/7 M urea gel and electrotransferred onto a nylon membrane (MSI MagnaCharge; Osmonics). The same membrane was used for the three Northern blots shown in this figure by following the recommendations of the membrane manufacturer for stripping the probe. (*A*) Schematic of the *glyW cysT leuZ* transcript. Numbers indicate the size (in nucleotides) of the spacer regions 5′ and 3′ of the *tRNA*^{Cys} gene. Hatched rectangles indicate the oligonucleotide probes. All oligonucleotide probes were 5′-end-labeled with [γ-^{32}P]ATP using T4 polynucleotide kinase. The diagram is not drawn to scale. (*B*) Processing of the 3′ end of tRNA^{Cys}. Northern analysis was done using an oligonucleotide probe (cysT–leuZ) complementary to the 12-nt spacer region between tRNA^{Cys} and tRNA^{Leu}. (*C*) Processing at the 5′ end of tRNA^{Cys}. The Northern blot was stripped and reprobed with oligonucleotide glyW–cysT complementary to a section of the 54-nt 5′ spacer region of tRNA^{Cys}. (*D*) Detection of the mature tRNA^{Cys} using the cysT probe. Sizes of selected bands are indicated on the right.

ases (RNase II, RNase BN, RNase D, RNase PH, RNase T, and PNPase) that have been shown to be involved in the generation of mature 3′ CCA termini (Li and Deutscher 1996) would be sufficient for maturation. To determine if this hypothesis were correct, we examined the processing of the *pheU* transcript because it contains 37 nt downstream of the mature CCA terminus (Fig. 6A) and it is almost identical in sequence organization to *pheV* (contains a 36-nt downstream sequence), the other phenylalanine tRNA in *E. coli*. Thus, analysis of the *pheU* transcript allowed us to simultaneously measure processing of both phenylalanine tRNAs.

To our surprise, the 116–117-nt-long primary transcript of tRNA^{Phe} was observed in all three *rne* mutant strains (Fig. 6B). Of even more interest were the longer half-lives for the *pheU/pheV* precursors compared with the polycistronic transcripts (e.g., Table 3, for *rne-1* cf. the half-lives of 31.8 min for the *pheU* and *pheV* precursors with 9.9 min for *cysT leuZ* and 14.5 min for *hisR leuT*). However, as was seen for the polycistronic operons, processing was significantly faster in the *rne*Δ*645* strain compared with either the *rne-1* or *rne*Δ*610* mutants (Table 3; Fig. 3D). No intermediates were detected in the *rne*$^+$ strain (Fig. 6B). When these experiments were repeated with the *rne*Δ*610* and *rne*Δ*645* alleles in single copy, the 116–117-nt *pheU/pheV* precursors were processed fivefold more rapidly in the *rne*Δ*645* strain compared with the *rne*Δ*610* mutant (data not shown).

Table 3. *Processing of polycistronic and monocistronic tRNA transcripts*

Transcript	Region	Half-life[a] (min)			
		rne$^+$	*rne-1*	*rne*Δ*610*	*rne*Δ*645*
glyW cysT leuZ	*cysT-leuZ*	ND	9.9 ± 0.5	7.0 ± 0.4	3.5 ± 0.7
	glyW-cysT[b]	ND	5.9	NC	NC
argX hisR leuT proM	*hisR-leuT*	ND	14.5 ± 1.9	15.0 ± 5.4	4.1 ± 0.1
	argX-hisR[b]	ND	12.5	10.4	3.4
pheU	*pheU* tRNA	ND	31.8 ± 5.0	20.2 ± 3.0	8.6 ± 3.1

[a]Half-lives were determined as the average of two independent experiments for the largest precursor detected (full-length) in each Northern blot. The various alleles were present in 6–8 copies/cell.
[b]Experiments were performed only once.
ND, No intermediates were detected.
NC, Half-lives were not calculated because of the low level of intermediates that were observed.

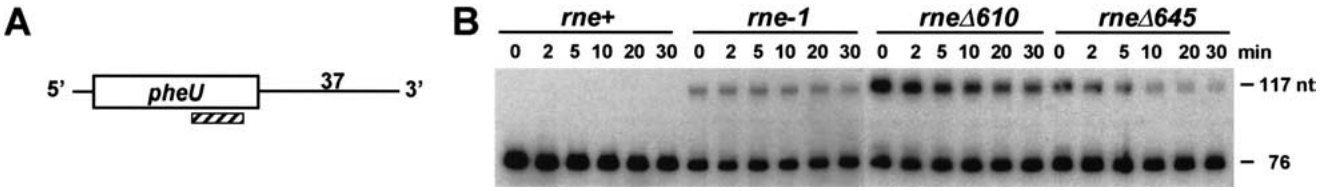

Figure 6. Processing of the *pheU* monocistronic transcript. The same conditions were used as described in Figure 5. (*A*) Schematic of the *pheU* monocistronic transcript. The hatched rectangle is the oligonucleotide probe (pheU2) complementary to the mature $tRNA^{Phe}$. The diagram is not drawn to scale. (*B*) Northern analysis using the pheU2 oligonucleotide probe to detect both the mature $tRNA^{Phe}$ as well as the unprocessed $tRNA^{Phe}$ precursor. The sizes of both species are indicated on the right.

To show that *pheU* and *pheV* were not unique among the monocistronic tRNA transcripts, we also examined the maturation of $tRNA^{Asn}$ under steady-state conditions. There are four copies of this gene in the *E. coli* genome (*asnT*, *asnU*, *asnV*, and *asnW*), each transcribed as a monocistronic transcript of a different length. Inactivation of RNase E led to a large increase in the amount of the four precursor tRNAs (see Fig. 9, below).

When we compared the differences in tRNA processing rates (Fig. 3D) with the variations in the mRNA decay half-lives (Fig. 3C) and the growth profiles at 44°C associated with the *rne-1*, *rne*Δ*610*, and *rne*Δ*645* strains (Fig. 3A,B), we observed a direct correlation between cell growth and tRNA-processing efficiency.

Maturation of the 5′ terminus of tRNA precursors requires prior RNase E cleavage

To determine if RNase E cleavage was the rate-limiting step in tRNA maturation, we performed two different types of experiments. Previous in vitro experiments by Ray and Apirion (1981a) suggested that the action of RNase E could influence RNase P cleavage at the 5′ terminus of an unprocessed tRNA transcript. Accordingly, to examine whether in vivo RNase P processing of the 5′ terminus was affected by RNase E cleavage at the 3′ end, we performed Northern analyses with probes designed to detect the presence of unprocessed 5′ termini. First, we tested for 5′-end processing of the *tyrT* tRNA, which is the first gene in the *tyrT tyrV tpr* transcript and contains a 44-nt 5′-terminal region (Fig. 7A). Although no processing intermediates were observed in the wild-type control, a variety of larger species were observed in the three *rne* mutants, indicating that RNase P cleavage required prior activity by RNase E at the 3′ end (Fig. 7B).

Although this result strongly suggested that RNase P did not process the 5′ end of the *tyrT* precursor prior to RNase E cleavage at the 3′ end, we wanted to confirm this observation using a simpler substrate. Accordingly, we examined the steady-state levels of six monocistronic transcripts (*asnT*, *asnU*, *asnV*, *ansW*, *pheU*, and *pheV*) in wild-type, *rne-1*, *rnpA49*, and *rne-1 rnpA49* strains after a 150-min shift to 44°C. In the case of $tRNA^{Asn}$, the four unprocessed monocistronic transcripts are 230 nt (*asnT*), 210 nt (*asnW*), and 120 nt (*asnU* and *asnV*) in length (Figs. 8A, 9). Each transcript contains ~9–10 nt upstream of the mature 5′ end. In an *rnpA49* mutant, which encodes a temperature-sensitive mutation in the protein subunit of RNase P (Apirion and Gitelman 1980), there was a large increase in an 85-nt species that represented all four $tRNA^{Asn}$ species that had been processed by RNase E at their 3′ ends but not by RNase P at their 5′ termini (Fig. 8A). In contrast, in the *rne-1* strain, the full-length precursors (230, 210, and 120 nt) accumulated. If RNase P functioned prior to RNase E cleavage, one would have expected to see species of ~220, ~200, and ~110 nt in the *rne-1* mutant. The fact that the $tRNA^{Asn}$ band profile in the *rnpA49 rne-1* double mutant was identical to those seen in the two single mutants further suggested that all potential processing intermediates were accounted for.

A similar result was obtained with the *pheU* and *pheV* transcripts (Fig. 8A). In this case, the full-length transcripts are 116 nt (*pheV*) and 117 nt (*pheU*), respectively, and contain a very short 5′ leader (3–4 nt). In the *rnpA49* mutant, two species (80–81 nt) differing in length by 1 nt accumulated, containing the immature 5′ end and 1–2

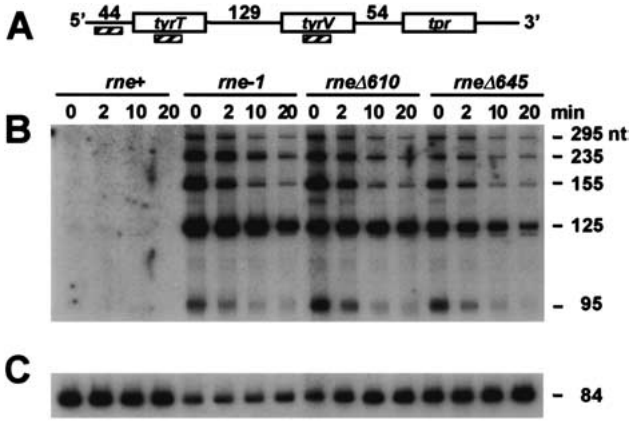

Figure 7. Processing of the *tyrT tyrV tpr* polycistronic transcript. The same procedures were followed as described in Figure 5. Hatched rectangles indicate the oligonucleotide probes. (*A*) Diagrammatic representation of the operon (not to scale). (*B*) Processing of the 5′-end *tyrT*. Northern analysis was done using primer tyrT5′A, which was specific for the entire 44-nt 5′ unprocessed terminus of *tyrT*. (*C*) Detection of the mature $tRNA^{Tyr}$ using primer tyrTV3′. The sizes of the various tRNA transcripts are indicated on the right.

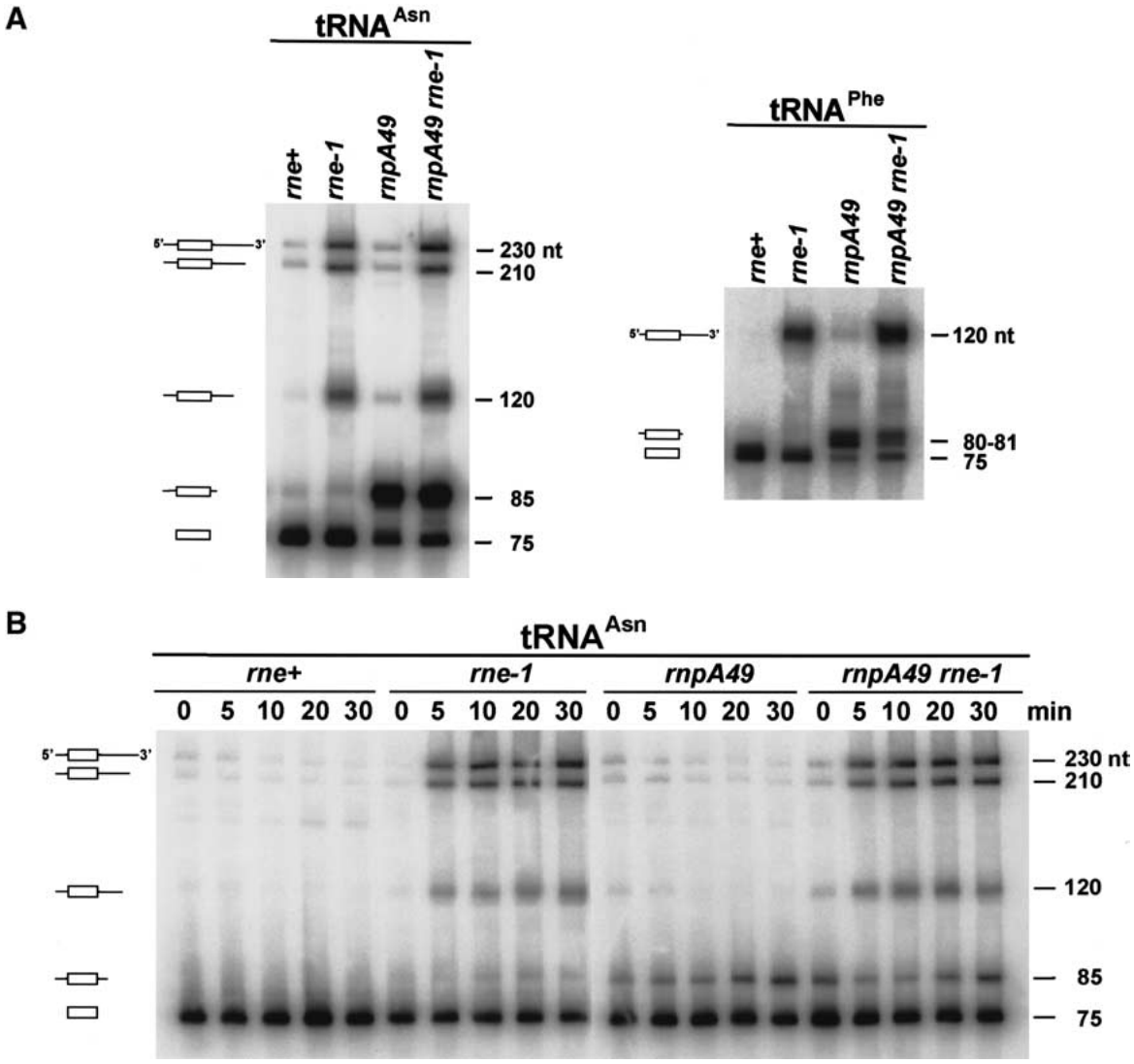

Figure 8. Analysis of tRNA processing in RNase E and RNase P mutants. (*A*) Steady-state RNA was isolated from each strain following a 150-min shift to 44°C as described in Materials and Methods. (*B*) Total RNA was isolated from cultures shifted to 44°C for the specified times. Five micrograms of total RNA was loaded into each lane of a 6% polyacrylamide/7 M urea gel. Each blot was probed with an oligonucleotide complementary to the mature tRNA. Diagrams of the tRNA species are shown on the left. The sizes on the right were determined using RNA molecular size standards (Invitrogen).

extra nucleotides at the 3′ end. In contrast, in the *rne-1* mutant, only the full-length transcripts accumulated. Again, there was no evidence for an intermediate that contained a mature 5′ end and an immature 3′ end.

Although the steady-state analysis indicated that RNase P processing of tRNA precursors did not occur prior to RNase E cleavage, we also performed kinetic experiments with both $tRNA^{Asn}$ (Fig. 8B) and $tRNA^{Phe}$ (data not shown) following a shift to 44°C. At the time of the shift, the mature $tRNA^{Asn}$ was the major species in the *rne*$^+$ and *rne-1* strains (Fig. 8B). In the *rnpA49* mutant there was also a low level of the 85-nt product, indicating that RNase P activity was slightly defective at 30°C. In the *rnpA49 rne-1* double mutant, there were higher levels of all the precursors. More importantly, in the *rne-1* strain the four full-length $tRNA^{Asn}$ transcripts accumulated over time, whereas the 85-nt species containing the unprocessed 5′ ends rapidly appeared in the *rnpA49* strain. With the *rnpA49 rne-1* double mutant, all of the precursors accumulated following the shift to 44°C (Fig. 8B). The kinetic analysis confirmed the results obtained with the steady-state experiment (Fig. 8A).

Analysis of tRNA processing efficiency at 44°C

In our Northern analysis of various tRNA transcripts, we noticed considerable differences in the half-lives among the various tRNA precursors (Table 3), suggesting a possible hierarchy of substrates for RNase E, whereby some were cleaved more efficiently than others. Accordingly, we examined the steady-state levels of 59 tRNA transcripts in the *rne*$^+$, *rne-1*, *rne*Δ*610*, and *rne*Δ*645* strains at

44°C under conditions such that each allele was present in 6–8 copies/cell. These experiments showed that there were three classes of tRNA substrates for RNase E. One group (Class 1) including $tRNA^{Asn}$ (Fig. 9), $tRNA^{Val}$, $tRNA^{Tyr}$, $tRNA^{Gly}$, $tRNA^{Phe}$, and $tRNA^{Met}$ were very efficiently processed in the *rne*$^+$ strain such that between ~95% and ~99% of the tRNA was present in the mature form (PF) under steady-state conditions. At the other extreme (Class 3), $tRNA^{His}$ (Fig. 9), $tRNA^{Cys}$, and $tRNA^{Arg}$ were inefficiently processed such that only ~28%–30% of the transcripts were mature in the wild-type strain under identical conditions. Class 2, represented by $tRNA^{Pro}$ (Fig. 9), $tRNA^{Glt}$, and $tRNA^{Leu}$, had PF values that ranged between 75% and 85%. Similar differences in PF values were observed when the *rne* alleles were present in single copy (data not shown).

Significant differences among the PF values for the various tRNAs were also observed in the *rne-1*, *rne*Δ*610*, and *rne*Δ*645* mutants (Fig. 9; data not shown). For example, the PF in the *rne-1* strain was always lower than that obtained in the *rne*$^+$ control. In the case of $tRNA^{His}$, there was a 14-fold reduction, whereas with $tRNA^{Pro}$ the decrease was 2.8-fold (Fig. 9). In addition, the PF was always greater in the *rne*Δ*645* strain compared with the *rne-1* and *rne*Δ*610* mutants (Fig. 9; data not shown). Furthermore, irrespective of their relative processing efficiencies, the steady-state amounts (RQ) of each tRNA were always *rne*$^+$ > *rne*Δ*645* > *rne*Δ*610* ≥ *rne-1*. This relationship correlated well with the growth profiles of these strains at 44°C (Fig. 3A,B). These data were also in complete agreement with the relative tRNA precursor half-lives described in Figure 3D.

Mapping RNase E cleavage sites within tRNA precursors

Because RNase E appeared to play an integral role in the processing of all the 59 tRNA transcripts we tested, we carried out a series of primer extension experiments to map some of the actual cleavage sites. When we tested the *tyrT* transcript, there was a single cleavage site located 1 nt downstream of the mature CCA terminus (CCAU↓AAUUCACC; Table 4; Fig. 10). This result was confirmed by performing a Northern blot for *tyrT* using steady-state RNA isolated from a Δ*rnt::kan rph-1* strain (SK10148), which should not be able to generate a mature 3′ end because of the loss of RNase T and RNase PH (Li and Deutscher 1994, 1996). No large precursors were observed, but an ~86-nt species, 1 nt longer than the mature $tRNA^{Tyr}$, was present in significant amounts (data not shown). In a second experiment, we determined the RNase E cleavage site between the *lysY* and *lysZ* genes. In this case, cleavage also occurred 1 nt downstream of the mature CCA terminus (CCAG↓UUUUA ACA; Table 4).

Because both of the RNase E cleavage sites mapped very close to the mature CCA terminus and fell within an AU-rich region, we decided to compare the downstream sequences of the three classes of tRNAs identified by the experiments described in Figure 9. In particular, we wanted to see if there were any correlations between those tRNAs that were processed inefficiently (*his*, *cys*, and *arg*) and those that were processed efficiently (*asn*, *val*, *tyr*, *gly*, and *met*). As shown in Table 4, most of the 3′ regions are AU-rich. In general, in the efficiently processed tRNAs there is usually an A residue

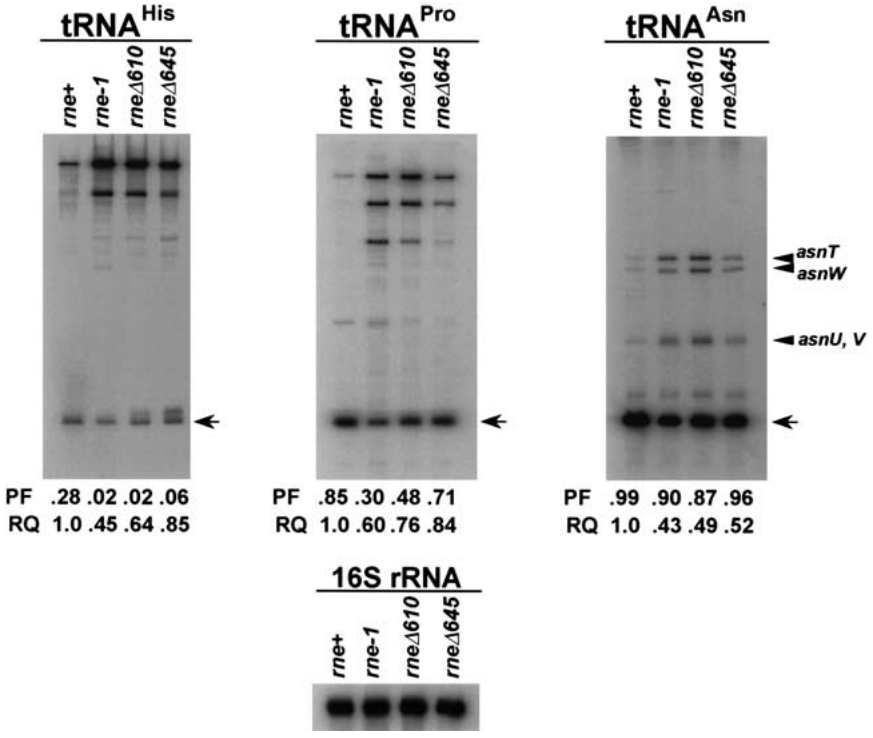

Figure 9. Analysis of steady-state levels of tRNAs in various RNase E mutants. Steady-state RNA was isolated from SK9714 (*rne*$^+$) and SK9937 (*rne-1*) after cultures had been shifted to 44°C for 120 min as indicated in Materials and Methods. For SK9957 (*rne*Δ*610*) and SK9987 (*rne*Δ*645*), the cultures were grown for 240 min prior to isolating RNA. The Northern blots were run as described in Figure 5. The membranes were probed with oligonucleotides complementary to either $tRNA^{His}$ (hisR), $tRNA^{Pro}$ (proM), $tRNA^{Asn}$ (asn), or 16S rRNA (rrnB2448). PF denotes the processed fraction that is defined as the amount of a given mature tRNA relative to the total amount of that tRNA (processed and unprocessed). RQ indicates the amount of mature tRNA in each lane compared with that determined in the *rne*$^+$ strain. As a normalization control a blot was probed for 16S rRNA.

immediately downstream of the CCA, but in those inefficiently processed there is either a C or a U (Table 4). However, the significance of this observation is called into question by the fact that some of the intermediately processed tRNAs like *leuV* have a 3′-terminal region that is almost identical to that of *metV* and *metZ* (Table 4). In addition, there are a number of 3′ ends such as *valZ* that appear to be processed efficiently but are GC-rich (Table 4).

Discussion

Although previous work by Apirion and coworkers has suggested a possible role for RNase E in tRNA maturation (Ray and Apirion 1981a,b), use of several RNase E mutants has permitted us to show that in vivo, tRNA processing is the likely reason that RNase E is essential for cell viability. In addition, we have presented evidence that RNase E is required for the processing of every possible type of tRNA transcript (monocistronic, polycistronic, and tRNAs contained within rRNA operons). Our results also confirm that RNase E cleavage is the rate-limiting step in the maturation of tRNAs.

Table 4. *Analysis of 3′ termini of various tRNA transcripts*

tRNA gene	3′ terminal region[a]	Processing efficiency[b]
tyrT	**CCA**U↓AAUUC	High
lysY	**CCA**G↓UUUUA	High
metZ	**CCA**AUUAAA	High
metW	**CCA**AUCAAA	High
metV	**CCA**AUUAUU	High
asnV	**CCA**AAUUCA	High
asnW	**CCA**AAUUUU	High
asnU	**CCA**AAUUCC	High
asnT	**CCA**AAUUCU	High
glyW	**CCA**GUUUAA	High
glyV	**CCA**AAAUUU	High
pheU	**CCA**AAUUCA	High
pheV	**CCA**CUAAUU	High
valZ	**CCA**UCGG↑GU	High
hisR	**CCA**UUAUUA	Low
cysT	**CCA**CUUUCU	Low
argX	**CCA**UUUAGU	Low
argV	**CCA**UAUUCU	Low
argY	**CCA**UCUCUU	Low
argZ and *argQ*	**CCA**UAUUCU	Low
argU	**CCA**UUACAA	Low
argW	**CCA**UUUAUC	Low
leuT	**CCA**CGACUU	Intermediate
leuV	**CCA**AUUAUC	Intermediate
proM	**CCA**AUUUUG	Intermediate

[a]The mature CCA terminus is shown in bold. Known RNase E cleavage sites are indicated by the downward arrows. In the case of *valZ,* the RNase P cleavage site is given since the mature *lysY* 5′ end starts 4 nucleotides downstream of the *valZ* CCA sequence.

[b]Processing efficiency is defined based on the observations described in Figure 9. High (Class 1) represents those tRNAs that are processed very efficiently (e.g., $tRNA^{Asn}$) in wild-type *E. coli.* Low (Class 3) are those tRNAs that are processed inefficiently (e.g., $tRNA^{His}$) under identical conditions. Intermediate (Class 2) are those tRNAs (e.g., $tRNA^{Pro}$) that are processed at intermediate levels.

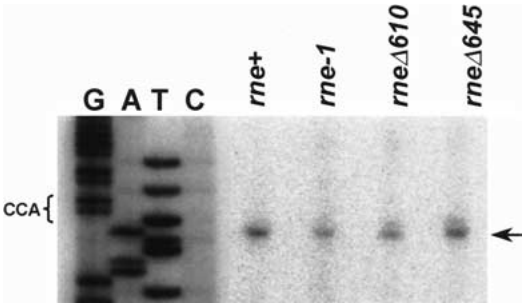

Figure 10. Primer extension analysis of *tyrT*. Two micrograms of total steady-state RNA from SK9714 (*rne*$^+$), SK9937 (*rne-1*), SK9957 (*rne*Δ*610*), or SK9987 (*rne*Δ*645*) was subjected to primer extension analysis using a ^{32}P-end-labeled primer (tyrTV) complementary to a segment of the spacer region between *tyrT* and *tyrV*. RNA from SK9714 and SK9937 was isolated after a 120-min shift to 44°C, whereas RNA from SK9957 and SK9987 was isolated after a 240-min shift as described in Materials and Methods. The primer extension product, mapping 1 nt after the CCA terminus (Table 4), is indicated by the arrow. A sequencing ladder obtained by using the same primer is shown at the left.

What is the evidence to support these conclusions? In the first place, even though RNase E is involved in the processing of 9S rRNA, the M1 subunit of RNase P, and the degradation of a large number of mRNAs, the data presented (Tables 1,2; Figs. 3C,4) show that these pathways are affected similarly in the *rne-1*, *rne*Δ*610*, and *rne*Δ*645* mutants, irrespective of their growth properties at 44°C (Fig. 3A,B). In contrast, the defects in tRNA processing and the relative amounts of mature tRNAs present in the *rne-1*, *rne*Δ*610*, and *rne*Δ*645* mutants directly correlated with their ability to grow at 44°C (Figs. 3A,B,D, 5–7, 9; Table 3).

With each allele present in 6–8 copies/cell, the *rne-1* strain ceased growing between 1–2 h after the shift to 44°C, whereas it took the *rne*Δ*610* mutant 3–4 h to stop growing. On the other hand, the *rne*Δ*645* strain continued to grow with a slightly longer generation time than the wild-type control (Fig. 3A). If one now compares the half-lives of the precursor tRNA transcripts at 44°C (Table 3), the processing reactions catalyzed by RNase E were most impaired in the *rne-1* strain, followed closely by the *rne*Δ*610* mutant. The processing of the three tRNA substrates tested was between 2.0- and 3.7-fold faster in the *rne*Δ*645* strain compared with the *rne*Δ*610* parent (Table 3; Fig. 3D). These changes were far greater than any differences observed in mRNA decay (Table 1; Fig. 3C), M1 processing (Table 2), or 9S rRNA processing (Fig. 4). For example, the processing of the 9S rRNA precursor was identical, within experimental error, in both the *rne*Δ*610* and *rne*Δ*645* strains (Fig. 4). In addition, the half-life of the M1 precursor of RNase P was indistin-

guishable in the *rne-1* and *rne*Δ*645* strains (Table 2). In the case of mRNA decay, although only three specific transcripts were tested, in all cases the half-lives in the *rne*Δ*645* temperature-resistant revertant were either comparable to or longer than those observed in the temperature-sensitive *rne-1* strain at 44°C (Table 1B; Fig. 3C). When the *rne* mutations were present in single copy, a similar correlation between growth at 44°C and tRNA processing rates was also observed (data not shown).

Furthermore, the levels of mature tRNAs in the three mutants were in the order of *rne*Δ*645* > *rne*Δ*610* ≥ *rne-1* (Fig. 9; data not shown). Thus, one would expect the *rne-1* strain to experience a shortage of tRNAs at 44°C far more quickly than the *rne*Δ*610* or *rne*Δ*645* strains, leading to the more rapid cessation of cell growth that was observed (Fig. 3A). Additional support for this conclusion comes from the fact that when the copy number of *rne*Δ*610* was reduced, the growth properties of the *rne*Δ*610* and *rne-1* strains were almost identical (Fig. 3B) and the half-lives of the *pheU*/*pheV* precursors were now longer than those observed in the *rne-1* mutant (data not shown).

The analysis of the 5′ termini of tRNA precursors either by examining their degradation (Fig. 7) or the identification of tRNA processing intermediates in mutants defective in either RNase E or RNase P (Fig. 8), confirmed previous results (Ray and Apirion 1981a; Li and Deutscher 2002) that generation of the mature 5′ terminus by RNase P cleavage required prior processing by RNase E. For example, in the case of the *asn* tRNAs, there are four different monocistronic transcripts that all contain 9–10 nt at the 5′ end but vary in length because of differences at their 3′ termini. Inactivation of RNase P would be expected to result in the accumulation of a single species that contained the unprocessed 5′ end of each $tRNA^{Asn}$ and a few extra nucleotides at the 3′ terminus. In fact, a species of 85 nt was the most prominent species in the *rnpA49* mutant (Fig. 8A). In the *rne-1* strain, two types of precursor were possible: the full-length transcripts of 230, 210, and 120 nt, or processed intermediates that lacked their 5′ leaders but retained their unprocessed 3′ ends (220, 200, and 110 nt). Only the larger species were observed (Fig. 8). Similar results were seen for *pheU*, *pheV* (Fig. 8A), and *met* (data not shown). It thus appears that 5′ maturation is absolutely dependent on initial cleavages at the 3′ end by RNase E. As such, the inviability observed in RNase E mutants may be partially an indirect effect of preventing RNase P cleavage at the 5′ end of individual tRNAs.

Our results also suggest that RNase E is probably involved in the processing of all tRNAs, because we observed an effect on all 59 of the transcripts that we tested. These included the four *glt* tRNAs, which are contained in four different rRNA operons. What was of interest was that the tRNAs fell into three groups. The first group were those that were processed efficiently ($tRNA^{Asn}$), such that ~95%–99% of the steady-state tRNA existed in the mature form in the wild-type control (Fig. 9; Table 4). In comparison, there was a second group, exemplified by $tRNA^{His}$ (Fig. 9; Table 4), that were inefficiently processed whereby ~28%–30% of the tRNA existed in the mature form in the wild-type control. The third class of tRNAs ($tRNA^{Pro}$; Fig. 9; Table 4) were processed with an intermediate level of efficiency. However, in all cases, the relative amount of mature tRNA was greater in the temperature-resistant *rne*Δ*645* strain compared with either the temperature-sensitive *rne-1* or *rne*Δ*610* mutants (Fig. 9; data not shown).

Taken together, these data indicate that tRNA processing in *E. coli* involves a series of steps that require initial cleavage events in the 3′ terminal regions by RNase E. Subsequently, RNase P and the various 3′ → 5′ exonucleases can complete the maturation process. Our results support the model for maturation of polycistronic tRNAs that was recently published (Li and Deutscher 2002) while this paper was in preparation. In addition, because RNase E also is required to process monocistronic tRNAs (Fig. 6), it is apparent that the multiple 3′ → 5′ exonucleases involved in generating the mature CCA terminus (Li and Deutscher 1994, 1996) normally do not remove more than a few nucleotides at the 3′ termini of tRNAs.

Several interesting questions are raised by the data reported here. One relates to the recognition of various substrates by RNase E. In all three *rne* mutants (*rne-1*, *rne*Δ*610*, and *rne*Δ*645*), tRNA processing was impaired compared with the wild-type control (Figs. 5–7, 9). The main differences among the three strains were the rate with which they processed the precursor transcripts (Table 3) and the fraction of mature tRNA in the total steady-state RNA population (Fig. 9). However, even though both the *rne-1* and *rne*Δ*610* strains stopped growing at 44°C (Fig. 3A,B), 9S rRNA processing was almost normal in the *rne*Δ*610* mutant (Fig. 4). In contrast, the decay of mRNAs in the *rne*Δ*610* and *rne*Δ*645* strains was far more defective at 37°C than in the *rne-1* mutant at 44°C (Table 1A,B; Ow et al. 2000). At 44°C, some of the differences were even more striking (Table 1B). Thus, RNase E appears to have different binding affinities for 9S rRNA versus mRNAs. In addition, based on the wide range of processing rates (Table 3) and the differences observed in steady-state levels (Fig. 9), some tRNAs are better substrates than others.

What can account for these differences? Ehretsmann et al. (1992) proposed a 5-nt recognition site for RNase E. Subsequent work has suggested that only a single-stranded AU-rich region is necessary (Cohen and McDowall 1997). By these criteria, however, it is not possible to distinguish why the *tyrT* processing site (CCAU↓AAUUC; Table 4; Fig. 10) is cleaved very efficiently but the *hisR* sequence (CCAUUAUUA) is not. In addition, examination of the 3′ termini of the three classes of tRNA substrates (Table 4) shows that the vast majority of them are AU-rich. It would, therefore, appear that secondary and tertiary structures must play an important role in site recognition.

Another point regards the nature of the *rne*Δ*645* allele. Isolated as a revertant of the already extensive RNase E truncation mutant *rne*Δ*610*, *rne*Δ*645* encodes an even

shorter polypeptide than its progenitor (Figs. 1,2). Surprisingly, this revertant was able to grow at 44°C, albeit at a slower rate than the *rne*$^+$ strain, in both 6–8 copies/cell and in single copy (Fig. 3A,B). Although the *rne*Δ*645* mutation was initially isolated from a putative *rng::cat rne*Δ*610* double mutant, we have subsequently obtained additional *rne*Δ*645*-like alleles in the *rne*Δ*610* genetic background (data not shown).

Of most interest was that an even shorter version of the RneΔ610 protein could suppress the lethality observed at 44°C. A computer search using the amino acids missing in RneΔ645 (418–427; ser leu ser leu ser ile leu arg leu ile) did not yield any known motifs that would explain why the additional truncation generates a protein that is now able to maintain cell viability. The loss of the additional 35 amino acids could change the structure of the protein, resulting in an enzyme that more effectively processes tRNAs, hence rescuing the temperature sensitivity of the *rne*Δ*610* parental strain. Interestingly, *rne*Δ*645* is a recessive mutation (data not shown). Solving the crystal structure of RNase E would help explain this puzzle as well as aid investigators in defining how the various domains of RNase E interact with RNA substrates.

It is now clear that RNase E plays an important role in all aspects of RNA processing and decay in *E. coli*, including rRNAs, tRNAs, mRNAs, and catalytic RNAs. It is thus somewhat surprising that only the N-terminal catalytic domain of the protein has been evolutionarily conserved and that some organisms such as *Bacillus subtilis* do not even contain an RNase E homolog (Kaberdin et al. 1998).

Materials and methods

Bacterial strains and plasmid displacement

The *E. coli* strains used in this study are listed in Table 5. Strains SK2525, SK2534, SK2681, SK2685, SK9982, SK9987, SK10103, SK10143, SK10144, and SK10148 were constructed by a combination of P1 transduction and plasmid displacement (Ow et al. 2000, 2002). Details of these constructions are available upon request.

Plasmid construction

The plasmids used are listed in Table 5. Vector pMOK18 was made by inserting an *Sma*I/*Sma*I streptomycin/spectinomycin-resistance cassette from pKRP13 (Reece and Phillips 1995) into the *Sca*I site of pWSK29 (Wang and Kushner 1991). To make pMOK19 (*rne*Δ*610* Sm^r), a *Kpn*I/*Sac*I DNA fragment from pMOK15 (*rne*Δ*610* Cm^r; Ow et al. 2000) containing the *rne*Δ*610* allele was inserted into the *Kpn*I/*Sac*I sites of pMOK18.

Table 5. E. coli *strains and plasmids*

Strain	Genotype[a]	Source or reference
MG1693	*rph-1*	*E. coli* Genetic Stock Center
SK2525	*rnpA49 rph-1 rbsD296::*Tn*10* Tc^r	This study
SK2534	*rnpA49 rne-1 rph-1 rbsD296::*Tn*10* Tc^r	This study
SK2681	*rne*Δ*1018::bla rph-1 srlD300::*Tn*10 recA56* Tc^r/pDHK2 (*rne*Δ*610* Sm^r/Sp^r)/pWSK129 (Km^r)	This study
SK2685	*rne*Δ*1018::bla rph-1 srlD300::*Tn*10 recA56* Tc^r/pDHK6 (*rne*Δ*645* Sm^r/Sp^r)/;WSK129 (Km^r)	This study
SK9714	*rne*Δ*1018::bla rph-1 recA56 srlD300::*Tn*10* Tc^r/pSBK1 (*rne*$^+$ Cm^r)	(Ow et al. 2000)
SK9937	*rne*Δ*1018::bla rph-1 recA56 srlD300::*Tn*10* Tc^r/pMOK13 (rne-1 Cm^r)	(Ow et al. 2000)
SK9957	*rne*Δ*1018::bla rph-1 recA56 srlD300::*Tn*10* Tc^r/pMOK15 (*rne*Δ*610* Cm^r)	(Ow et al. 2000)
SK9982	*rne*Δ*1018::bla rng::cat rph-1 recA56 srlD300::*Tn*10* Tc^r/pMOK19 (*rne*Δ*610* Sm^r/Sp^r)	This study
SK9987	*rne*Δ*1018::bla rph-1 recA56 srlD300::*Tn*10* Tc^r/pMOK21 (*rne*Δ*645* Sm^r/Sp^r)	This study
SK10103	*rne*Δ*1018::bla rph-1 recA56 srlD300::*Tn*10* Tc^r/pMOK29 (*rne*Δ*645* Cm^r)	This study
SK10143	*rne*Δ*1018::bla rph-1 srlD300::*Tn*10 recA56* Tc^r/pMOK44 (*rne*$^+$ Sp^r)/pWSK129 (Km^r)	(Ow et al. 2002)
SK10144	*rne*Δ*1018::bla rph-1 srlD300::*Tn*10 recA56* Tc^r/pMOK45 (*rne-1* Sp^r)/pWSK129 (Km^r)	This study
Sk10148	*rph-1* Δ*rnt::kan* Km^r	This study

Plasmids	Genotype	Source or reference
PKRP13	High-copy plasmid with Sm^r/Sp^r	(Reece and Phillips 1995)
pWSK29	6–8 copy plasmid with Ap^r	(Wang and Kushner 1991)
pWSK129	6–8 copy plasmid with Km^r	(Wang and Kushner 1991)
pMOK15	6–8 copy plasmid with *rne*Δ*610* Cm^r	(Ow et al. 2000)
pMOK18	6–8 copy plasmid with Sm^r/Sp^r	This study
pMOK19	6–8 copy plasmid with *rne*Δ*610* Sm^r/Sp^r	This study
pMOK21	6–8 copy plasmid with *rne*Δ*645* Sm^r/Sp^r	This study
pMOK29	6–8 copy plasmid with *rne*Δ*645* Cm^r	This study
pMOK40	Single-copy plasmid with Sm^r/Sp^r	(Ow et al. 2002)
pMOK44	Single-copy plasmid with *rne*$^+$ Sm^r/Sp^r	(Ow et al. 2002)
pMOK45	Single-copy plasmid with *rne-1* Sm^r/Sp^r	This study
pDHK2	Single-copy plasmid with *rne*Δ*610* Sm^r/Sp^r	This study
pDHK6	Single-copy plasmid with *rne*Δ*645* Sm^r/Sp^r	This study

[a]All strains contain the *thyA715* allele.

pMOK21 (*rne*Δ*645* Sm^r) was isolated naturally from a 44°C replica plate of SK9982. pMOK29 (*rne*Δ*645* Cm^r) was made using site-directed mutagenesis using pMOK15 as the template. Plasmids pDHK2 and pMOK45 were constructed by digesting pMOK15 (*rne*Δ*610*) and pMOK13 (*rne-1*), respectively, with *Sac*I and *Kpn*I and ligating the DNA fragment containing the *rne* mutant allele into a *Sac*I/*Kpn*I-digested pMOK40 (Sp^r) vector (Ow et al. 2002). pDHK6 was made by inserting an *Eco*RI/*Not*I fragment carrying the *rne*Δ*645* allele into the *Eco*RI/*Not*I sites in pMOK40.

Growth curves

Cultures were routinely grown in Luria broth with thymine (50 μg/mL) and chloramphenicol (20 μg/mL), kanamycin (50 μg/mL), spectinomycin (20 μg/mL), or streptomycin (20 μg/mL) at 37°C or 30°C with agitation until they reached 40–45 Klett units (1×10^8–1.1×10^8 cells/mL; No. 42 green filter). Once reaching this density, cultures were shifted to 44°C. Every 30 min thereafter, cells were diluted with fresh prewarmed medium. Klett values were adjusted with the appropriate dilution factor.

DNA sequencing

Sequencing of the *rne*Δ*645* allele was done using an ABI Prism 310 Genetic Analyzer (PE Applied Biosystems) as instructed by the manufacturer using primers RNE+240, RNE+292, RNE+747, RNE+1006, and RNE+3628. These primers encompassed the *rne*Δ*610* and *rne*Δ*645* genes in their entirety.

Site-directed mutagenesis

The introduction of a stop codon into plasmid pMOK15 (*rne*Δ*610*) to generate the *rne*Δ*645* allele (pMOK29) was done with the U.S.E. Mutagenesis Kit (Amersham Pharmacia) following the instructions of the manufacturer. The selection and the mutagenesis primers (which convert the codon for serine 418 from TCG to a TAG stop codon) were RNE-893 and RNE+1593T, respectively. DNA sequencing at the site of the C → A transversion and RNase E Western blot analysis on strain SK10103 were performed to verify the authenticity of the mutation.

Western analysis

Western analysis was performed as described previously (Ow et al. 2000, 2002).

Primer extension analysis

Primer extensions were carried out using Thermoscript RNase H$^-$ reverse transcriptase (Invitrogen) at 60°C according to the manufacturer's specifications. The sequences for the various primers used in the hybridization reactions are available upon request.

Northern analysis

For RNA isolation and Northern analysis, we followed the procedures described in O'Hara et al. (1995) and Burnett (1997). All of the RNAs used for the tRNA-processing Northern blots were obtained from 44°C cultures diluted as described for the growth curves so the cultures were maintained in exponential growth at all times. RNA was obtained from exponentially growing cultures that had been shifted to 44°C for 2 h (SK9937) and 4 h (SK9714, SK9957, and SK9987). These times were chosen based on the times after shift at which the *rne-1* and *rne*Δ*610* strains stopped growing (Fig. 3A). The 9S rRNA Northern was done using RNA extracted from cultures shifted to 44°C for 150 min. For strains carrying single copies of *rne-1*, *rne*Δ*610*, and *rne*Δ*645* and the *rnpA49* and *rnpA49 rne-1* mutants, RNA was isolated after a 150-min shift to 44°C. RNAs from MG1693 (*rph-1*) and SK10148 (Δ*rnt::kan rph-1*) were harvested from exponentially growing cultures at 37°C. Band densities were quantitated with a Phosphorimager series 400 (Molecular Dynamics). Decay rates for half-life determinations were calculated using linear regression analysis.

Acknowledgments

This work was supported in part by a grant from the NIGMS (GM57220) to S.R.K. M.C.O. was supported in part by a NIH predoctoral traineeship from NIGMS (GM07106). We are thankful to M. Wachi and S. Lovett for providing strains. We also thank B. Mohanty and T. Perwez for critical readings of the manuscript and R. Fabbri and D.-H. Chung for technical assistance.

The publication costs of this article were defrayed in part by payment of page charges. This article must therefore be hereby marked "advertisement" in accordance with 18 USC section 1734 solely to indicate this fact.

References

Altman, S., Kirsebom, L., and Talbot, S. 1995. Recent studies of RNase P. In *tRNA: Structure and function* (eds. D. Soll and Raj Bhandary), pp. 67–78. ASM Press, Washington, DC.

Apirion, D. and Gitelman, D. 1980. Decay of RNA in RNA processing mutants of *Escherichia coli*. *Mol. Gen. Genet.* **177:** 139–154.

Arraiano, C.M., Yancey, S.D., and Kushner, S.R. 1988. Stabilization of discrete mRNA breakdown products in *ams pnp rnb* multiple mutants of *Escherichia coli* K-12. *J. Bacteriol.* **170:** 4625–4633.

Babitzke, P. and Kushner, S.R. 1991. The Ams (altered mRNA stability) protein and ribonuclease E are encoded by the same structural gene of *Escherichia coli*. *Proc. Natl. Acad. Sci.* **88:** 1–5.

Babitzke, P., Granger, L., and Kushner, S.R. 1993. Analysis of mRNA decay and rRNA processing in *Escherichia coli* multiple mutants carrying a deletion in RNase III. *J. Bacteriol.* **175:** 229–239.

Berlyn, M.K.B. 1998. Linkage map of *Escherichia coli* K-12, Edition 10: The traditional map. *Microbiol. Mol. Biol. Rev.* **62:** 814–984.

Burnett, W.V. 1997. Northern blotting of RNA denatured in glyoxal without buffer recirculation. *Bio. Techn.* **22:** 668–671.

Carpousis, A.J., Van Houwe, G., Ehretsmann, C., and Krisch, H.M. 1994. Copurification of *E. coli* RNAase E and PNPase: Evidence for a specific association between two enzymes important in RNA processing and degradation. *Cell* **76:** 889–900.

Casarégola, S., Jacq, A., Laoudj, D., McGurk, G., Margarson, S., Tempête, M., Norris, V., and Holland, I.B. 1992. Cloning and analysis of the entire *Escherichia coli ams* gene. *ams* is identical to *hmp-1* and encodes a 114 kDa protein that migrates as a 180 kDa protein. *J. Mol. Biol.* **228:** 30–40.

———. 1994. Cloning and analysis of the entire *Escherichia coli*

ams gene. *ams* is identical to *hmp1* and encodes a 114 kDa protein that migrates as a 180 kDa protein. *J. Mol. Biol.* **238:** 867.

Cohen, S.N. and McDowall, K.J. 1997. RNase E: Still a wonderfully mysterious enzyme. *Mol. Microbiol.* **23:** 1099–1106.

Ehretsmann, C.P., Carpousis, A.J., and Krisch, H.M. 1992. Specificity of *Escherichia coli* endoribonuclease RNase E: In vivo and in vitro analysis of mutants in a bacteriophage T4 mRNA processing site. *Genes & Dev.* **6:** 149–159.

Ghora, B.K. and Apirion, D. 1978. Structural analysis and in vitro processing to p5 (5S) rRNA of a 9S RNA molecule isolated from an *rne* mutant of *E. coli*. *Cell* **15:** 1055–1066.

Gurevitz, M., Jain, S.K., and Apirion, D. 1983. Identification of a precursor molecule for the RNA moiety of the processing enzyme RNase P. *Proc. Natl. Acad. Sci.* **80:** 4450–4454.

Hajnsdorf, E., Steier, O., Coscoy, L., Teysset, L., and Régnier, P. 1994. Roles of RNase E, RNase II and PNPase in the degradation of the *rpsO* transcripts of *Escherichia coli*: Stabilizing function of RNase II and evidence for efficient degradation in an *ams pnp rnb* mutant. *EMBO J.* **13:** 3368–3377.

Jain, C. and Belasco, J.G. 1995. RNase E autoregulates its synthesis by controlling the degradation rate of its own mRNA in *Escherichia coli*: Unusual sensitivity of the *rne* transcript to RNase E activity. *Genes & Dev.* **9:** 84–96.

Kaberdin, V.R., Miczak, A., Jakobsen, J.S., Lin-Chao, S., McDowall, K.J., and von Gabain, A. 1998. The endoribonucleolytic N-terminal half of *Escherichia coli* RNase E is evolutionarily conserved in *Synechocystis* sp. and other bacteria but not the C-terminal half, which is sufficient for degradosome assembly. *Proc. Natl. Acad. Sci.* **95:** 11637–11642.

Li, Z. and Deutscher, M.P. 1994. The role of individual exoribonucleases in processing at the 3′ end of *Escherichia coli* tRNA precursors. *J. Biol. Chem.* **269:** 6064–6071.

———. 1996. Maturation pathways for *E. coli* tRNA precursors: A random multienzyme process in vivo. *Cell* **86:** 503–512.

———. 2002. RNase E plays an essential role in the maturation of *Escherichia coli* tRNA precursors. *RNA* **8:** 97–109.

Liu, F. and Altman, S. 1995. Inhibition of viral gene expression by the catalytic RNA subunit of RNase P from *Escherichia coli*. *Genes & Dev.* **9:** 471–480.

López, P.J., Marchand, I., Joyce, S.A., and Dreyfus, M. 1999. The C-terminal half of RNase E, which organizes the *Escherichia coli* degradosome, participates in mRNA degradation but not rRNA processing in vivo. *Mol. Microbiol.* **33:** 188–199.

Lundberg, U. and Altman, S. 1995. Processing of the precursor to the catalytic RNA subunit of RNase P from *Escherichia coli*. *RNA* **1:** 327–334.

Mackie, G.A. 1991. Specific endonucleolytic cleavage of the mRNA for ribosomal protein S20 of *Escherichia coli* requires the products of the *ams* gene in vivo and in vitro. *J. Bacteriol.* **173:** 2488–2497.

———. 1998. Ribonuclease E is a 5′-end-dependent endonuclease. *Nature* **395:** 720–723.

Miczak, A., Kaberdin, V.R., Wei, C.-L., and Lin-Chao, S. 1996. Proteins associated with RNase E in a multicomponent ribonucleolytic complex. *Proc. Natl. Acad. Sci.* **93:** 3865–3869.

Mudd, E.A., Krisch, H.M., and Higgins, C.F. 1990. RNase E, an endoribonuclease, has a general role in the chemical decay of *Escherichia coli* mRNA: Evidence that *rne* and *ams* are the same genetic locus. *Mol. Microbiol.* **4:** 2127–2135.

O'Hara, E.B., Chekanova, J.A., Ingle, C.A., Kushner, Z.R., Peters, E., and Kushner, S.R. 1995. Polyadenylation helps regulate mRNA decay in *Escherichia coli*. *Proc. Natl. Acad. Sci.* **92:** 1807–1811.

Ono, M. and Kuwano, M. 1979. A conditional lethal mutation in an *Escherichia coli* strain with a longer chemical lifetime of mRNA. *J. Mol. Biol.* **129:** 343–357.

Ow, M.C., Liu, Q., and Kushner, S.R. 2000. Analysis of mRNA decay and rRNA processing in *Escherichia coli* in the absence of RNase E-based degradosome assembly. *Mol. Microbiol.* **38:** 854–866.

Ow, M.C., Liu, Q., Mohanty, B.K., Andrew, M.E., Maples, V.F., and Kushner, S.R. 2002. RNase E levels in *Escherichia coli* are controlled by a complex regulatory system that involves transcription of the *rne* gene from three promoters. *Mol. Microbiol.* **43:** 159–171.

Py, B., Causton, H., Mudd, E.A., and Higgins, C.F. 1994. A protein complex mediating mRNA degradation in *Escherichia coli*. *Mol. Microbiol.* **14:** 717–729.

Py, B., Higgins, C.F., Krisch, H.M., and Carpousis, A.J. 1996. A DEAD-box RNA helicase in the *Escherichia coli* RNA degradosome. *Nature* **381:** 169–172.

Ray, B.K. and Apirion, D. 1981a. RNAase P is dependent on RNAase E action in processing monomeric RNA precursors that accumulate in an RNAase E$^-$ mutant of *Escherichia coli*. *J. Mol. Biol.* **149:** 599–617.

———. 1981b. Transfer RNA precursors are accumulated in *Escherichia coli* in the absence of RNase E. *Eur. J. Biochem.* **114:** 517–524.

Reece, K.S. and Phillips, G.J. 1995. New plasmids carrying antibiotic-resistance cassettes. *Gene* **165:** 141–142.

Régnier, P. and Hajnsdorf, E. 1991. Decay of mRNA encoding ribosomal protein S15 of *Escherichia coli* is initiated by an RNase E-dependent endonucleolytic cleavage that removes the 3′ stabilizing stem and loop structure. *J. Mol. Biol.* **187:** 23–32.

Taraseviciene, L., Miczak, A., and Apirion, D. 1991. The gene specifying RNase E (*rne*) and a gene affecting mRNA stability (*ams*) are the same gene. *Mol. Microbiol.* **5:** 851–855.

Vanzo, N.F., Li, Y.S., Py, B., Blum, E., Higgins, C.F., Raynal, L.C., Krisch, H.M., and Carpousis, A.J. 1998. Ribonuclease E organizes the protein interactions in the *Escherichia coli* RNA degradosome. *Genes & Dev.* **12:** 2770–2781.

Wang, R.F. and Kushner, S.R. 1991. Construction of versatile low-copy-number vectors for cloning, sequencing and expression in *Escherichia coli*. *Gene* **100:** 195–199.